Computing the volumetric Mueller matrix with in-line holography

Maria J. Lopera[1,2,*], Maciej Trusiak[3], Ana Doblas[4], Yunfeng Nie[2], Heidi Ottevaere[2], Carlos Trujillo[1]
[1]*Applied Optics Group, School of Applied Science and Engineering, Universidad EAFIT, Medellín, Colombia.*
[2]*Brussels Photonics, Department of Applied Physics and Photonics, Vrije Universiteit Brussel and Flanders Make, Pleinlaan 2, B-1050 Brussels, Belgium.*
[3]*Warsaw University of Technology, Institute of Micromechanics and Photonics, 8 Sw. A. Boboli St., 02-525 Warsaw, Poland.*
[4]ECE Department, University of Massachusetts Dartmouth, New Bedford, Massachusetts 02747, USA.
mloper23@eafit.edu.co – maria.josef.lopera.acosta@vub.be

ABSTRACT
This study introduces an innovative approach to volumetric polarimetry, introducing a method that combines Gabor in-line holography with conventional polarimetric setups to compute the complete Mueller Matrix of a sample. The study includes the validation of the technique through calibration targets and extends to complex volumetric samples, showcasing the potential of this method for characterizing intricate polarization properties in three-dimensional specimens.

Keywords: Volumetric polarimetry, Mueller Matrix, Polarization, In-line holography

1. INTRODUCTION

In the field of Mueller matrix recovery, achieving complete volumetric retrieval remains a persistent challenge[1 2]. This research introduces an innovative alternative that harnesses the power of in-line Gabor holography to extract polarization information from volumetric samples. The proposed polarization-sensitive in-line holographic setup enables the recovery of the complete Mueller matrix of three-dimensional (3D) samples through a series of numerical retro-propagations of the holographically rendered complex wavefield to various sample planes[3]. The validation of this approach includes a calibrated birefringent polarization test target and two volumetric samples, one containing calcium oxalate crystals and another one containing polyethylene terephthalate (PET) plastics. The proposed method allows a detailed exploration of 3D polarimetric parameters, such as polarizance and retardance. What sets this proposed in-line Gabor holographic system apart is its sensitivity to axial variations in polarimetric information within volumetric samples. All of this is achieved without the need for mechanical movement or optical adjustments—a feature that has remained elusive to conventional image-plane reference methods and non-holographic/interferometric systems. The outcome of this study underscores the versatility and potential of this alternative approach, offering a groundbreaking avenue for recovering the intricate polarization characteristics of 3D specimens. Importantly, to the best of the authors' knowledge, it marks the first report of in-line holographic Mueller imaging.

2. IN-LINE POLARIMETRIC MICROSCOPY

The proposed method integrates an in-line microscopy system [4,5] with a complete polarimeter [6]. The in-line microscopy system employs plane illumination directed at the sample $S(\overrightarrow{r_0})$, with a microscope objective generating an intermediate magnified image $S(\overrightarrow{r_i})$. This image is propagated at a distance z until it reaches the sensor, following the principles of in-line holography. The polarimeter component begins with a linearly polarized light source before the sample, utilizing a Polarization States Generator (PSG) composed of a half-wave plate (λ/2) and a quarter-wave plate (λ/4). After passing through the sample and microscope objective, the light reaches the Polarization States Analyzer (PSA), consisting of a quarter-wave plate (λ/4) followed by a linear polarizer (LP). The PSG and PSA together enable the creation of degenerate polarization states of light (linear vertical: V, linear horizontal: H, linear +45: P, linear -45: M, right circular: R, left circular: L).

Unconventional Optical Imaging IV, edited by Irene Georgakoudi, Marc P. Georges, Nicolas Verrier, Proc. of SPIE Vol. 12996, 129960C · © 2024 SPIE · 0277-786X · doi: 10.1117/12.3017065

To fully retrieve the Mueller matrix of a sample, a total of 36 images are required. For each polarization state *d,* a hologram $I_d(\vec{r_{i'}}, z)$ is captured at the intermediate image plane $\vec{r_{i'}}$. Figure *1* provides a visual schematic of the setup.

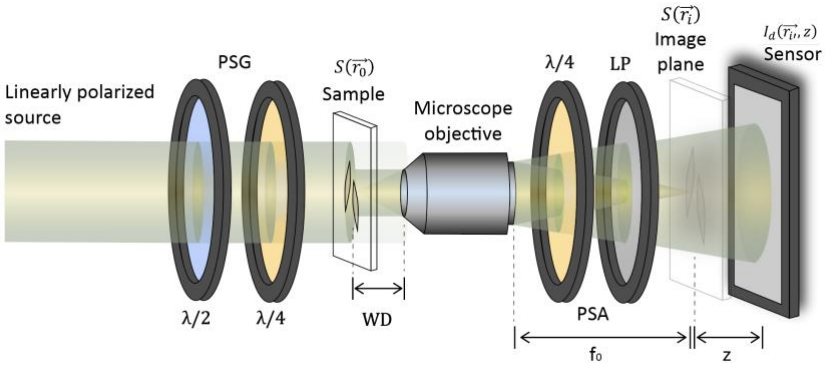

Figure 1. Scheme of the in-line polarimetric setup.

After acquiring the holograms, a numerical propagation using the Angular Spectrum algorithm [5] is conducted to retrieve the intensity of the field. This intensity is computed as the square magnitude of the retrieved field. Utilizing the obtained intensities, the Mueller matrix of the sample is constructed. The Mueller matrix, defined as a 4×4 matrix, encapsulates how the sample influences the polarization of incoming light, a process described by the Mueller calculus [3,7]. The Mueller matrix is defined as

$$M_u(\vec{r_i} \cdot M) = \begin{bmatrix} m_{00} & m_{01} & m_{02} & m_{03} \\ m_{10} & m_{11} & m_{12} & m_{13} \\ m_{20} & m_{21} & m_{22} & m_{23} \\ m_{30} & m_{31} & m_{32} & m_{33} \end{bmatrix} \quad (1)$$

Each of the coefficients in Eq. (*1*) is composed by the addition or subtraction of four of the retrieved intensities, described as shown in equations (*2*).

$$\begin{aligned} m_{00} &= HH + HV + VH + VV & m_{01} &= HH + HV - VH - VV \\ m_{02} &= PP + PV - MH - MV & m_{03} &= RH + RV - LH - LV \\ m_{10} &= HH - HV + VH - VV & m_{11} &= HH - HV - VH + VV \\ m_{12} &= PH - PV - MH + MV & m_{13} &= RH - RV - LH + LV \\ m_{20} &= HP - HM + VP - VM & m_{21} &= HP - HM - VP + VM \\ m_{22} &= PP - PM - MP + MM & m_{23} &= RP - RM - LP + LM \\ m_{30} &= HR - HL + VR - VL & m_{31} &= HR - HL - VR + VL \\ m_{32} &= PR - PL - MR + ML & m_{33} &= LL - RL - LR + RR \end{aligned} \quad (2)$$

3. RESULTS

The initial validation of the technique involves computing the retardance of a commercial birefringent test target (Thorlabs R2L2S1B)[8], which is specified by the manufacturer to induce an overall retardance of 280 nm at 532 nm. Figure *2* illustrates five vertical lines reconstructed from the target. The retardance was computed using the polar decomposition Mueller matrix [9,10] method and measured over the sample, specifically within the section indicated by the dashed white lines of Figure *2*. The average measured retardance with the proposed method was found to be 271 ± 14 nm. Despite the presence of noise artifacts stemming from the inherent diffraction process in the imaging technique, primarily affecting background information, the overall retardance values are accurately retrieved. The results depicted in *Figure 2* exhibit a remarkable alignment with the expected values, considering the system's 3.2% margin of error in these measurements.

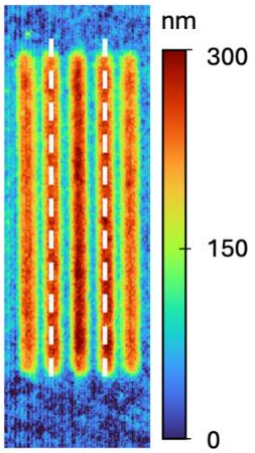

Figure 2. The retardance map measured with the proposed in-line polarimetric holographic technique for the commercial birefringent test target.

A second validation involves the examination of a volumetric sample. Specifically, a sample containing calcium oxalate crystals was prepared, with sediment fixed on both sides of a microscope slide. The axial distance between planes containing information on both sides of the slide is 1.5 *mm*. *Figure 3* illustrates the reconstructed intensity, focusing on one side of the microscope slide in panels (a) and (b), and focusing on the other side in panels (c) and (d). Additionally, intensity reconstructions considering parallel polarization states (HH) are displayed in panels (a) and (c), while reconstructions with perpendicular polarization states (HV) are shown in panels (b) and (d). Calcium oxalate crystals are well-known for their optical activity and response to polarization imaging [11,12]. For this sample, two Mueller matrices were obtained, one for each focal plane.

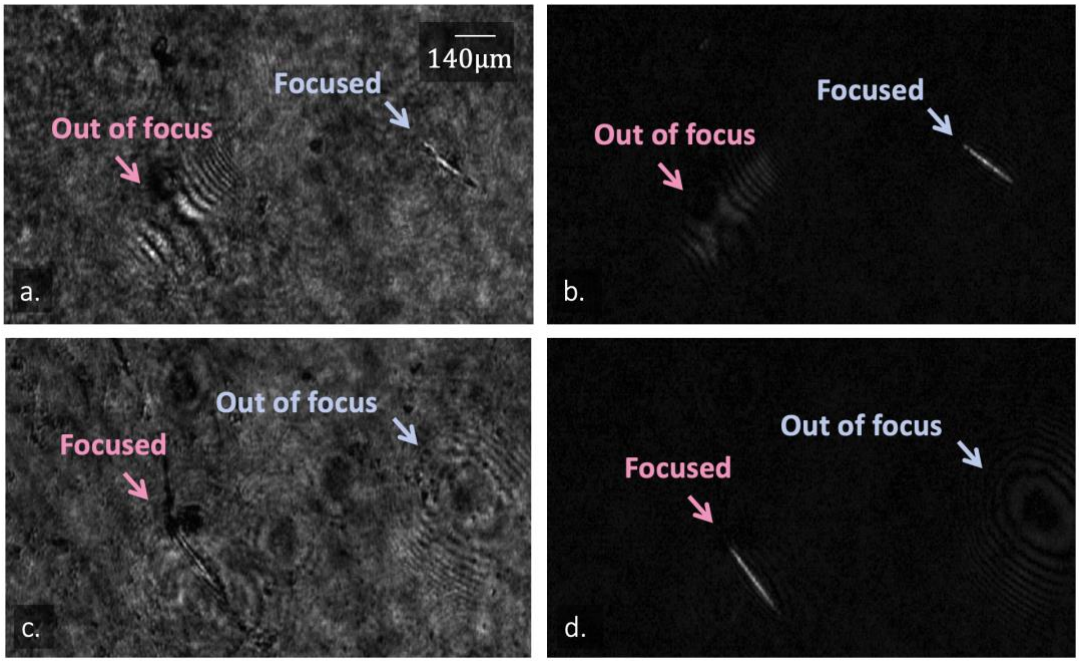

Figure 3. Parallel polarization states (HH) [a and c] and Perpendicular polarization states (HV) [b and d] images of a sample containing calcium oxalate crystals. Measurements on front side [a and b] and rear side [c and d] of the microscope slide containing the sample.

From each of the Mueller matrices, several observables can be computed. For this sample, the retardance (panels (a) and (b) of Figure *4*) and polarizance (panels (c) and (d)) are displayed. Within the dashed black squares, the value of the background is measured and contrasted to the value obtained for each of the crystals. The retardance of each crystal against its background is registered at approximately two radians. Additionally, concerning polarizance, the average value of the crystals observed for the crystals is roughly three times larger than the background value. These findings corroborate the sensitivity of the proposed method in detecting variations in both polarizance and retardance induced by samples exhibiting polarization-altering properties, such as the specimen chosen for this experiment.

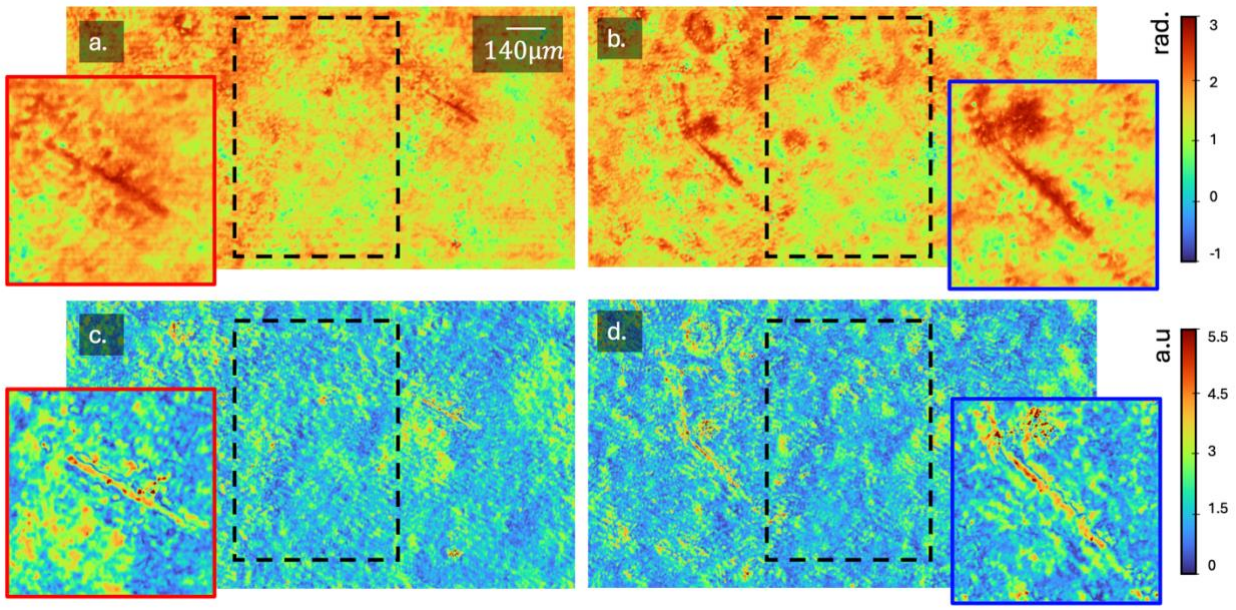

Figure 4. Measured retardance and polarizance maps of a sample containing Calcium Oxalate crystals over two different axial planes. Panels (a) and (c) are the metrics on the front side, while panels (b) and (d) in the rear side of the microscope slide.

For a final experiment, the same methodology is employed, utilizing a sample containing PET plastics positioned at different axial locations. Figure *5* illustrates the retardance and polarizance maps of the sample at these two distinct axial positions. As noted previously, the resulting maps exhibit diffraction artifacts, which can be effectively mitigated through numerical processing methods. However, despite these artifacts, the method can capture defined shapes of the objects at the two different reconstruction planes. This capability ensures a qualitative measurement of the imaged polarimetric variables, thus fully affirming the method's efficacy in providing volumetric imaging of polarization properties in the examined samples.

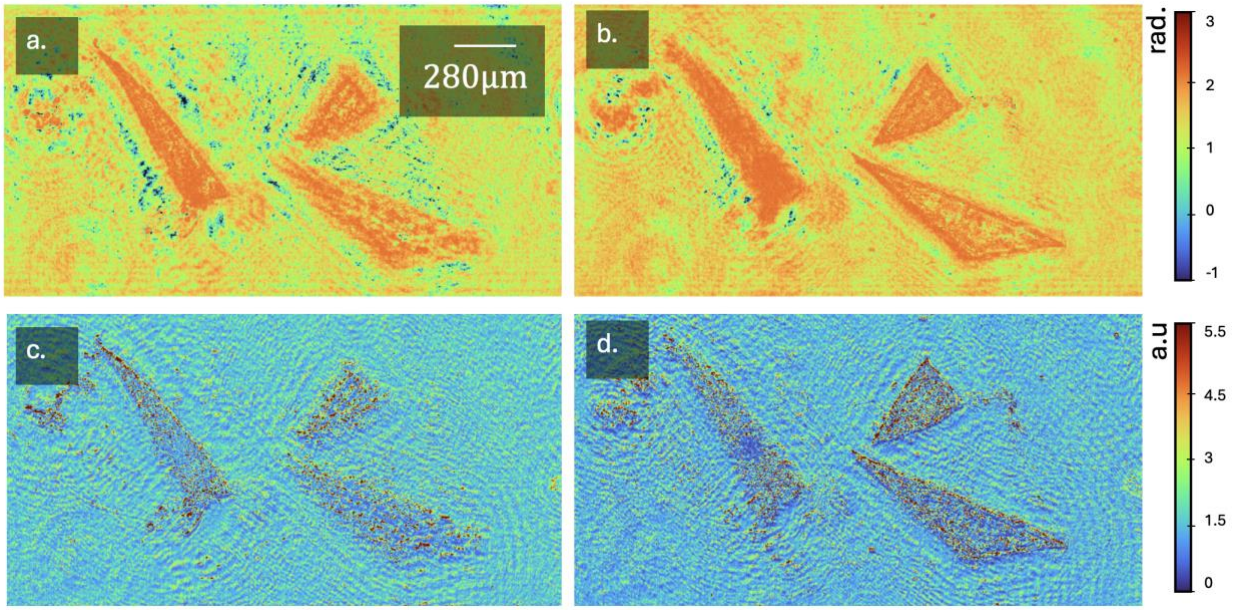

Figure 5. Measured retardance and polarizance maps of a sample containing PET plastic particles over two different axial planes. Panels (a) and (c) are the metrics in one plane, while panels (b) and (d) are in the other one.

4. CONCLUSIONS

The integrated approach combining in-line holographic microscopy with a complete polarimeter has proven to be effective in characterizing the optical properties of diverse samples. Through the utilization of Mueller matrix analysis, the retardance and polarizance have been successfully computed, providing valuable insights into the samples' behavior under polarized light. Notably, in the case of retardance measurements on a commercially available retardance test target, the close alignment between measured and anticipated values (within a 3.2% margin of error) underscores the accuracy and reliability of the method.

Furthermore, the significance of this approach is demonstrated by its capability to extract polarimetric data across varied axial positions, effectively capturing volumetric information. This capability is demonstrated through the retrieval of polarimetric information at different axial positions of the inspected samples, with measured values consistently agreeing with anticipated outcomes as reported in the literature.

Overall, the results presented in this paper highlight the versatility and applicability of the approach, showcasing its potential to provide comprehensive insights into the optical properties of a wide range of samples.

ACKNOWLEDGMENTS

The authors acknowledge the National Science Center Poland (OPUS 2020/37/B/ST7/03629), the Flemish Fund for Scientific Research (FWO) (11PGG24N, 1252722N), Global-MINDS (VLIR-UOS), the Methusalem and Hercules foundations, and the OZR of the Vrije Universiteit Brussel (VUB), and the support provided by Vicerrectoría de Ciencia, Tecnología e Innovación from Universidad EAFIT.

REFERENCES

[1] Lopera, M. J. and Trujillo, C., "Linear diattenuation imaging of biological samples with digital lensless holographic microscopy," Appl Opt **61**(5), B77 (2022).

[2] Nomura, T. and Kobata, T., "Digital holographic three-dimensional Mueller matrix imaging," Applied Optics, Vol. 54, Issue 17, pp. 5591-5596 **54**(17), 5591–5596 (2015).

[3] Lopera, M. J., Trusiak, M., Doblas, A., Ottevaere, H. and Trujillo, C., "Mueller-Gabor holographic microscopy," SSNR (2023).

[4] Micó, V., García, J., Zalevsky, Z. and Javidi, B., "Phase-shifting gabor holographic microscopy," IEEE/OSA Journal of Display Technology **6**(10), 484–489 (2010).
[5] Molony, K. M., Hennelly, B. M., Kelly, D. P. and Naughton, T. J., "Reconstruction algorithms applied to in-line Gabor digital holographic microscopy," Opt Commun **283**(6), 903–909 (2010).
[6] Obando-Vasquez, S., Doblas, A. and Trujillo, C., "Apparatus and method to recover the Mueller matrix in bright-field microscopy," Am J Phys **90**(9), 702–714 (2022).
[7] Collett, E., [Field Guide to Polarization, Volume FG0], SPIE Field Guides, Washington (2005).
[8] Thorlabs., "Thorlabs NBS 1963A Birefringent Resolution Target," 2023, <https://www.thorlabs.com/newgrouppage9.cfm?objectgroup_id=4338&pn=R2L2S1B> (18 September 2023).
[9] Boulvert, F., Le Brun, G., Le Jeune, B., Cariou, J. and Martin, L., "Decomposition algorithm of an experimental Mueller matrix," Opt Commun **282**(5), 692–704 (2009).
[10] Lu, S.-Y., Chipman, R. A., Lu, S.-Y. and Chipman, R. A., "Interpretation of Mueller matrices based on polar decomposition," J. Opt. Soc. Am. A **13**(5) (1996).
[11] Asselman, M., Verhulst, A., De Broe, M. E. and Verkoelen, C. F., "Calcium Oxalate Crystal Adherence to Hyaluronan-, Osteopontin-, and CD44-Expressing Injured/Regenerating Tubular Epithelial Cells in Rat Kidneys," Journal of the American Society of Nephrology **14**(12), 3155–3166 (2003).
[12] Gou, J., Shen, T. H., Bao, P., Ramos Angulo, J. L. and Evans, S. D., "A stokes polarimetric light microscopy view of liquid crystal droplets," Scientific Reports 2021 11:1 **11**(1), 1–9 (2021).